We are IntechOpen, the world's leading publisher of Open Access books Built by scientists, for scientists

6,900
Open access books available

186,000
International authors and editors

200M
Downloads

Our authors are among the

154
Countries delivered to

TOP 1%
most cited scientists

12.2%
Contributors from top 500 universities

WEB OF SCIENCE™

Selection of our books indexed in the Book Citation Index in Web of Science™ Core Collection (BKCI)

Interested in publishing with us?
Contact book.department@intechopen.com

Numbers displayed above are based on latest data collected.
For more information visit www.intechopen.com

Chapter

Mixed 2D-3D Halide Perovskite Solar Cells

Alaa E. Abd El-Samad, Radwa S. Mostafa, Hager H. Zeenelabden, Menahtullah M. Mabrouk, Ahmed Mourtada Elseman, Nasr Gad, Mostafa El-Aasser and Mohamed M. Rashad

Abstract

The 3D-perovskite halides have gained a considerable reputation versus their counterpart semiconductor materials since they achieved a remarkable high-power conversion efficiency of 25.2% within a decade. Perovskite solar cells also have some problems as lattice degradation and sensitivity against moisture, oxygen, and strong irradiation. The perovskite instability is the drawback in front of this emerging technology towards mass production and commercialization. 2D-perovskites, with the general formula $A_2B_{n-1}M_nX_{3n+1}$, have been recently introduced to overcome some of the drawbacks of the stability of 3D-perovskites; however, this is at the expense of sacrificing a part of the power conversion efficiency. Mixed 2D/3D perovskites could solve this dilemma towards the way to high stability-efficiency perovskites. The research is expected to obtain highly stable and efficient mixed 2D/3D perovskite solar cells in the few coming years. This chapter reviews 2D-perovskites' achieved progress, highlighting their properties, current trends, challenges, and future prospects.

Keywords: 2D, 3D, perovskite solar cells, stability, efficiency

1. Introduction

Perovskites are among the essential material science topics in the last decades due to their low-cost, solution-processed devices and exceptional optoelectronic properties [1–28]. The most studied compositions are represented by the formula ABX_3 (organic cation A is larger than the metal cation B, and X is a halide anion). For example, methylammonium lead tri-iodide ($CH_3NH_3PbI_3$ or $MAPbI_3$), the other halide variants such as $CH_3NH_3PbBr_3$ and mixed halides, $CH_3NH_3PbI_{3-x}Cl_x$ [29–31]. The most advantages of 3D-perovskite ($CH_3NH_3PbI_3$) are combining direct bandgap with high molar extinction coefficient ($\approx 10^4$–10^5 M^{-1} cm^{-1}), low trap densities, low exciton binding energies (≈10–50 meV), which cause long-range free-carrier diffusion lengths (≈100 nm). The perovskite is unique in such a way that its efficiency boosted up from 3.8% to 23.7% in just few years as compared to all other types of traditional solar cells. However, the lack of durability of these materials (hydrophilic cations) due to thermal instability and degradation upon exposure to humidity, U.V. radiation, and the electric field is still a significant barrier to

commercialization [32–34]. 3D-perovskite solar cells' performance decreases due to ion migration and segregation, the ionic nature of the materials, and their low formation energies, making them vulnerable to water-induced hydrolysis [35]. The instability issues associated with perovskite materials have been overcome by using additives, introducing intermediate phases, encapsulating the layers (to avoid spreading Pb toxicity into the external environment), etc. [36–38]. Several studies have also shown that mixed cations and halides tend to enhance perovskites' stability and efficiency.

A 2D Ruddlesden–Popper perovskite has a general formula of $A_2B_{n-1}M_nX_{3n+1}$, where "A" represents a large-sized organic cation [39]. Incorporating a bulky organic cation (2D) into the 3D-perovskite layer's crystal lattice passivates the vulnerable 3D-perovskite against oxygen and moisture intrusion, resulting in enhanced stability while maintaining the efficiency of 3D-Perovskite solar cell [40]. 2D-perovskites are very stable but have larger bandgaps and higher exciton binding energies than 3D-perovskites. On the other hand, the exceptional stability under heat and light soaking conditions of low-dimensional perovskites makes them essential to protect the highly efficient 3D [41]. Phenyl ethyl ammonium iodide (PEAI) as a bulky cation in 2D-perovskite was investigated and fabricated as a layered 2D/3D structure demonstrating an impressive PCE 20.1% with 85% PCE retention after 800 h in ambient conditions by Cho et al. [40]. The perovskite absorber composition has been optimized using a 2D-perovskite, and stable performance over 12000 h without the HTM was observed [42].

The 2D-perovskite solar cells (PSCs) have shown superiority over 3D ones, such as improved stability towards humidity and light, improved processability, long-term durability, and higher chemical versatility. All this makes 2D-perovskites a promising alternative and one that has attracted substantial attention over the past few years. The ability of 2D-perovskites to incorporate bigger, less volatile, and generally hydrophobic organic cations; which makes the materials with improved thermal and chemical stability. Furthermore, the ability to use an enormous variety of organic cations and various metals, halides, and combinations of all of the above make this family of materials can be employed in different applications such as solar cells and others [43, 44]. Though there are several approaches to stabilize the 3D-perovskite, the most common one is cation tuning. The bigger cations beyond the Goldsmith tolerance limit produce low dimensional perovskites at least 2.5 eV, restricting photons conversion to less than 500 nm. 2D-perovskites are very stable, but unfortunately they have larger bandgaps and higher exciton binding energies (≈300 meV), penalizing output photovoltage and, therefore, the power conversion efficiencies [45, 46]. Improved instability in metal halide PSCs is one of the most interesting issues to open the door for them towards commercialization. The reduced-dimensional perovskites (RDPs) have shown increase in ambient and operating lifetimes of PSCs. In other words 2D/3D heterostructure PSCs consisting of a thin layer of RDPs a top and a 3D active layer, improved both stability and efficiency compared to pure 3D counterparts [31, 47, 48], as shown in **Figure 1(a)**. Indeed, 2D/3D engineering aimed to combine both advantages, namely the outstanding optoelectronic properties of the 3D-perovskite and the 2D Ruddlesden–Popper phase's high robustness. Recently, based on the 2D/3D heterostructured lead halide perovskites, high-efficiency stable PSCs with an average PCE of 17.5 ± 1.3% was demonstrated. The "post-burn-in" efficiency could be retained over 80% after the air's operation for 1000 h and encapsulated process for 4000 h. Therefore, the performances of PSCs are brought closer to meeting the commercial requirements [49].

In this chapter, the 2D, 3D, and 2D/3D hybrid systems for perovskites will be discussed, focusing on the crystal structure, optoelectronic properties, synthesis methods, and layer orientation. Finally, application in regular or inverted structure

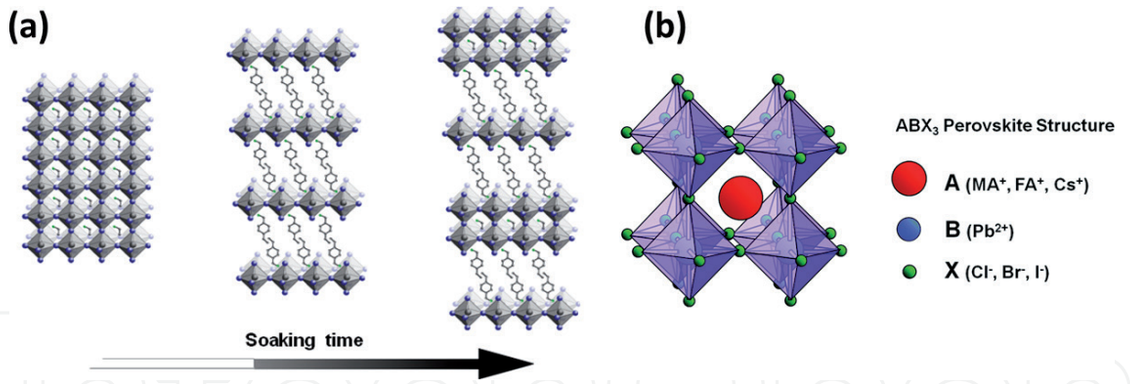

Figure 1.
(a) Dimensional mixed 2D/3D increases the soaking time and the stability of perovskite solar cells. Reprinted with permission from Ref. [31]. (b) The perovskite unit cell consists of an a cation (red) at the center, B cations in the corners (blue), and X anions (green) on the edges. The B cation forms an octahedral with the surrounding X anions (all eight octahedral are shown). Reprinted with permission from Ref. [50].

PSCs which remain to be addressed are herein highlighted while giving the outline on the perspectives of 3D and 2D/3D perovskites for high efficiency stable solar cells.

2. 3D-perovskites

2.1 Structures

Perovskite materials generally contain a cubic unit cell with the general formula ABX_3. Cation A, which is larger than cation B, is in the center of the unit cell. The B cations are in every corner of the unit cell; Cation B also serves as the center of an octahedron with an X anion surrounding cation B, corner-sharing between each cation B. As shown in **Figure 1(b)**, the full picture of cation A is surrounded by eight octahedra, each of which contains a cationic center B and anions X. In this orientation, the cubic structure of the perovskite has 6-fold the coordination number for cation A and 12-fold the coordination number for cation B. It should be noted that the ionic radii are quite crucial in maintaining a stable cubic unit cell.

2.2 Applications in regular or inverted structured perovskite solar cells

As mentioned, before we have n-i-p typical structure and p-i-n inverted structure. In 2018, Hua Dong et al. [51] applied $CH_3NH_3PbI_3$ film in highly efficient inverted planar heterojunction perovskite solar cells obtaining an efficiency of 17.04%. In 2020, Shuai Gu et al. [52] applied tin and mixed lead in tin halide perovskite tandem solar cells with a power conversion efficiency (PCE) over 25%.

2.3 Device fabrication methods

There are two ways to fabricate a PSC, solution and vacuum processing: (i) Spin coating is a solution deposition technique that uses high rotation speeds, as shown in **Figure 2(a** and **b)** [18, 26, 28]. A device rotates the substrate while a drop of the precursor solution is placed on the substrate. The high speed distributes the solution evenly on the substrate. After the material is deposited, the substrate is heated to evaporate and remove the solvent. This step is called the annealing step and the perovskite film is formed after removing the solvent. There are two methods of spin coating: a one-step and a two-step spin coating. In single-stage spin-coating, the

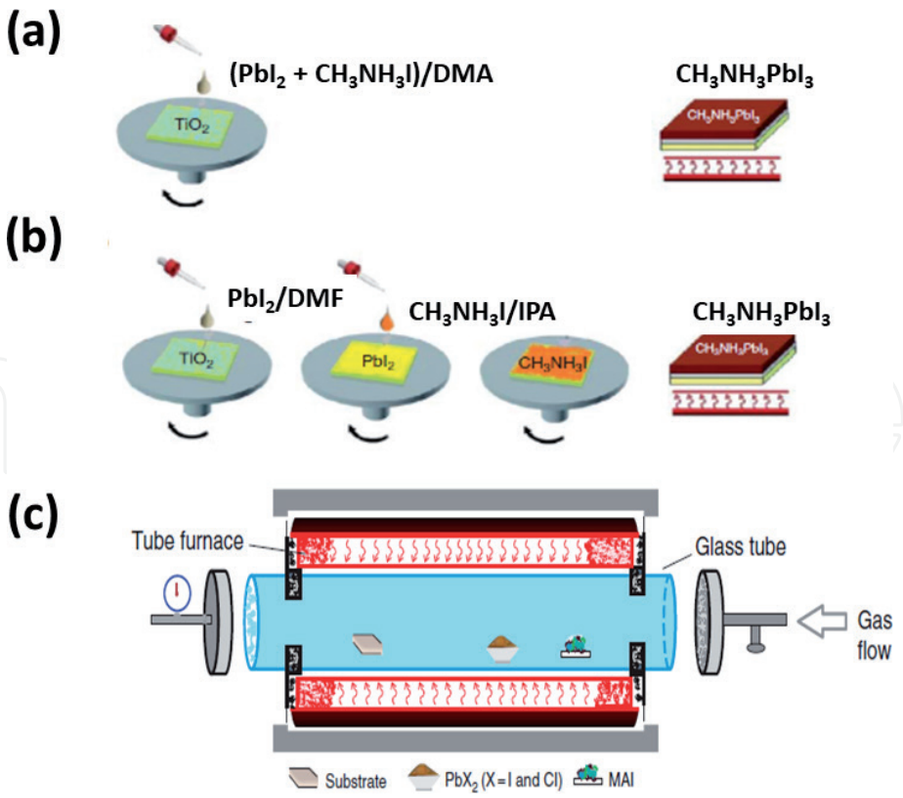

Figure 2.
(a) Method of one-step spin coating. (b) Method of two-step spin coating (c) a diagram of the CVD technique. Reprinted with permission from Ref. [53, 55]

solution contains all the chemicals deposited on the substrate. With a two-stage spin coating, organic and inorganic chemicals are deposited separately on the substrate. For example, $CH_3NH_3PbI_3$ perovskite material can be deposited onto a substrate by one-step or two-step spin-coating methods. In the one-step process, CH_3NH_3I and PbI_2 are mixed in solution with the solvent (dimethyl formamide (DMF)), and the solution is spin-coated onto the substrate. In the two-step method, PbI_2 is dissolved in the solvent (DMF) and spin-coated onto the substrate. Then, CH_3NH_3I is dissolved in the solvent (isopropanol (IPA)) and spin-coated onto the PbI_2-coated substrate [7, 53].

(ii) Vacuum treatment is a technique in which a CVD (Chemical Vapor Deposition) machine is used to achieve high temperatures in a glass housing [54]. Gases can flow through the pipe ends through the glass holder. This property is commonly used to achieve desired pressures or add reactive gas to the system. CVD has a temperature gradient along the tube so that the positions near the center are warmer than the positions near the ends of the tube. This temperature gradient is a critical aspect of the CVD manufacturing technique. The technology begins with the selection of the materials for the solar cell. The substrate is placed near the end of the tube and the materials for the solar cell are placed in a solid phase towards the center. When the CVD machine reaches the appropriate temperature, the solids in the center of the tube evaporate. An inert carrier gas such as argon flows through the tube and pushes the vaporized solids away from the substrate. The substrate has a lower temperature and causes condensation of the evaporated materials when they meet the substrate. This causes the materials to deposit on the substrate and form a thin layer. A diagram of the CVD technique is shown in **Figure 2(c)** [55].

The CVD technique can be used in several steps to deposit each material layer separately if desired. CVD technology has two distinct advantages over spin coating and other processes. First, the film layer produced is exceptionally clean since no solvent was used in the process, eliminating the possibility of impurities being

added to the solvent. Second, the process is relatively easy to scale up for large-scale manufacture. In addition, perovskite films produced with this technique have good uniformity, non-porous films, large grain sizes, and a long carrier life. Two parameters are used to optimize the vacuum deposition technique, deposition time and temperature. Deposition time determines the amount of material deposited on the substrate, so film thickness is the main effect of deposition time. The climate is essential for vacuum deposition technology. The temperature should be high enough to vaporize the materials, but most importantly, the temperature should not be high enough to melt the substrate. Adjusting the position of the substrate and solid materials in the tube will help heat the materials sufficiently and prevent the substrate from melting. However, the temperature and location of placement must be used together to achieve the desired results [56].

3. 2D-perovskites

Despite the high performance of the 3D-perovskite [57], which qualified it to be a strong competitor to the various other types of solar cells, the stability or the ability of 3D to resist various factors of humidity, heat, and so on represent a critical issue in the direction of the possibility of becoming commercial [48]. Although the researchers' focus was first on 3D, they turned to 2D to solve the stability problem that plagues 3D [58]. In the next section, we are going to talk about the structure of the 2D-perovskites, their optoelectronic properties, preparation methods, layers orientation, and applications in regular or inverted structure PSCs.

3.1 Structures

The general chemical formula of the 2D-perovskite is $A_2B_{n-1}M_nX_{3n+1}$, where A can be a monovalent or divalent organic cation that intercalates between the inorganic $An_{-1}B_nX_3n_{+1}$ 2D sheets works as a spacer between the inorganic cation as shown in **Figure 3(a)**. *n* is the thickness or the number of the inorganic layers and (n = 1 at the divalent A, and n = 2 at the monovalent A) [43].

2D-halide perovskite layers are conceptually obtained by cutting along the crystallographic planes <100>, <110> or < 111> of the 3D-perovskite structure [59] as shown in **Figure 3(b)**, so we can classify the 2D perovskite depending on cutting the shape of the 3D-perovskite into <100>, <110>, and < 111> – oriented perovskites. Cutting layers along <110> direction (can be derived from the face diagonal) and along <111> direction (can be derived from the body diagonal) are less common in 2D-halide perovskites. Unlike these two types, <100> perovskites are the most common type of 2D-halide perovskites and are commonly used in solar cells. The general formula of <100> – oriented 2D-perovskites is $A_2B_{n-1}M_nX_{3n+1}$, and their inorganic sheets are obtained by taking n-layers along the 100 direction of the 3D-perovskites. The <100> – oriented 2D-perovskites can be divided into two commonly used types. The first is Ruddlesden-Popper (R.P.), and the second is Dion-Jacobson (D.J.) [60, 61].

In Ruddlesden-Popper (R.P.), the most used and studied type (owing to its superior ambient stability [62]) has the chemical formula $A_2B_{n-1}M_nX_{3n+1}$. Each inorganic layer is confined between bilayers of bulky ammonium cations. The relatively weak van der Waals forces between the alkyl chains separating the layers generate a 2D structure. In 2017, Xiaoyan Gan and co-workers fabricated a 2D-perovskite $(PEA)_2(MA)_{n-1}Pb_nI_{3n+1}$ (phenylethylammonium = PEA, n = 1, 2, 3) with incorporation of TiO_2 nanorod arrays into a solar cell harvesting efficiency of 3.72% [60] with a structure of glass/FTO/TiO_2 as compact layer/$(PEA)_2(MA)_{m-1}Pb_mI_{3m+1}$/spiroO-MeTAD/Au as shown in **Figure 4**.

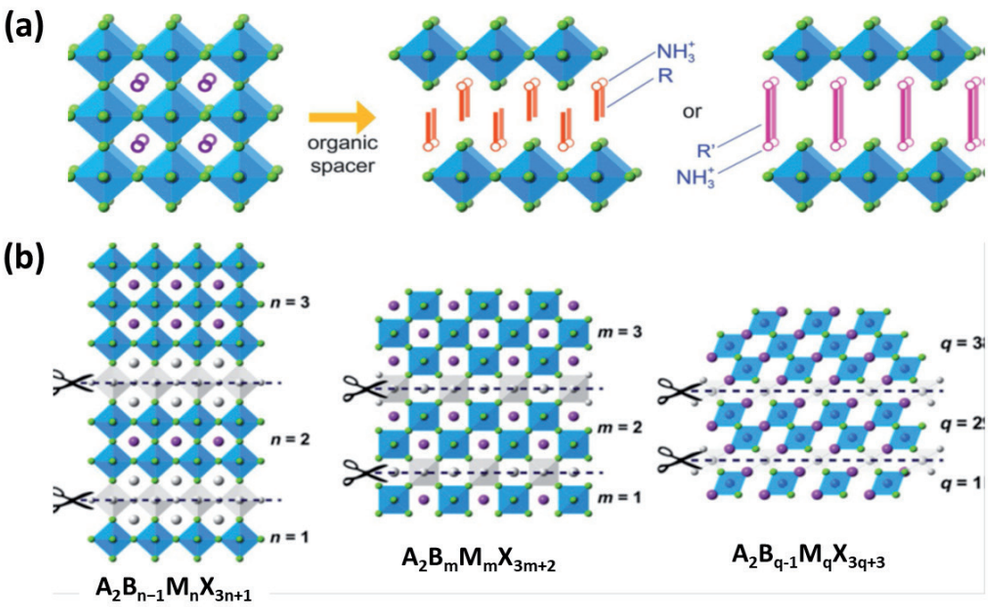

Figure 3.
(a) Crystal structures of a 3D-perovskite and the 2D-hybrid perovskite with monovalent and divalent ammonium cations. Reprinted with permission from Ref. [43]. (b) Cuts along <100>, <110> and < 111> directions and the 2D-perovskites that result from such cuts. Reprinted with permission from Ref. [43].

Dion–Jacobson (D.J.) perovskites adopt a general formula $AB_{n-1}M_nI_{3n+1}$. This type has layered structures where the stacking of inorganic layers is unique as they lay precisely on top of another, and this is quite the opposite of Ruddlesden-Popper (R.P.) [63]. The difference between R.P. and D.J. is shown in **Figure 5**.

In 2018, Sajjad Ahmad and co-workers developed a series of Dion-Jacobson phase 2D-perovskites that record a cell power conversion efficiency of 13.3% with high stability. Unencapsulated devices retain over 95% efficiency upon exposure to ambient air (40–70% relative humidity [R.H.]) for 4,000 hours, damp heat (85°C and 85% R.H.) for 168 hours, and continuous light illumination for 3,000 hours. This device is more stable than the R.P. counterpart, as shown in **Figure 6**. The

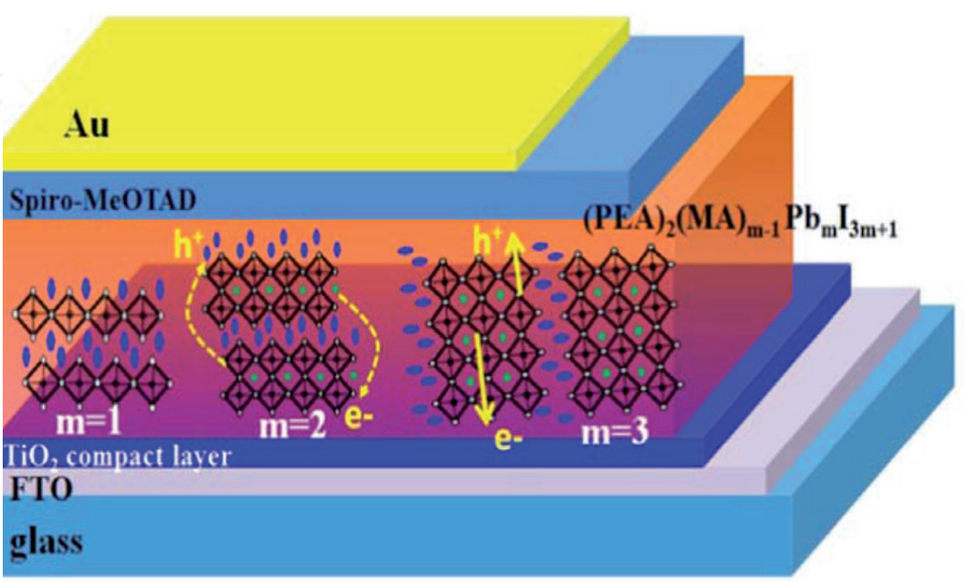

Figure 4.
A schematic device architecture of planar $(PEA)_2(MA)_{m-1}Pb_mI_{3m+1}$ based perovskite solar cell, consisting of glass/FTO/TiO_2CL/$(PEA)_2(MA)_{m-1}Pb_mI_{3m+1}$/spiroOMeTAD/Au. Reprinted with permission from Ref. [60].

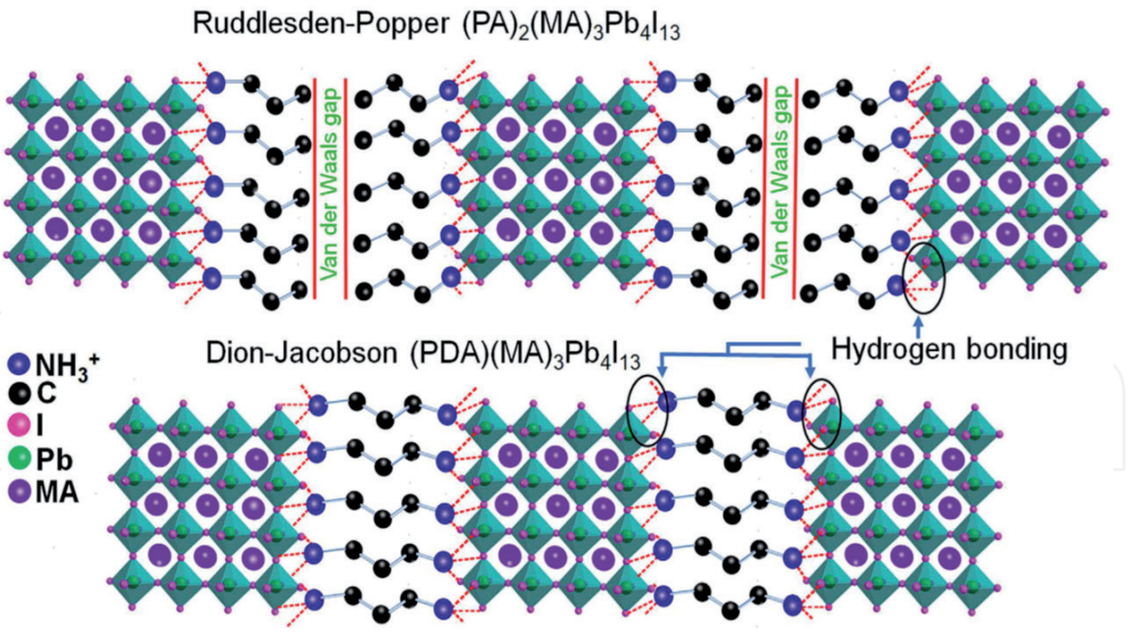

Figure 5.
Illustration of R.P. and D.J. phase 2D-layered perovskites. Reprinted with permission from Ref. [64].

improved device stability over the R.P. counterpart is attributed to alternating hydrogen bonding interactions between diammonium cations and inorganic slabs, strengthening the 2D-layered perovskite structure [64].

3.2 Applications in regular or inverted structure perovskite solar cells

The 2D-perovskites have many applications; it is used in solar cells, light emitting diodes, etc. Here we will concentrate on their applications in the n-i-p normal structure and p-i-n inverted structure solar cells as follows: In 2015, Cao and co-workers fabricated a 2D-perovskite thin-film and recorded an efficiency of 4.02% with a regular structure n-i-p with a device structure FTO/TiO_2/2D perovskite/spiro-OMeTAD/Au [65]. In 2016, Hsinhan Tsai and co-workers reported a photovoltaic efficiency of 12.52% with no hysteresis for an inverted structure solar cell FTO/PEDOT:PSS/$(BA)_2(MA)_3Pb_4I_{13}$/PCBM/Al [66]. In 2018, Xinqian Zhang and co-workers fabricated a vertically orientated highly crystalline 2D $(PEA)_2(MA)_{n-1}Pb_nI_{3n+1}$, n = 3, 4, 5) films with the assistance of an ammonium thiocyanate (NH_4SCN) additive. Planar-structured PSC with the device structure of ITO/PEDOT:PSS/$(PEA)_2(MA)_4Pb_5I_{16}$ (n = 5)/$PC_{61}BM$/BCP/Ag was fabricated. They got an efficiency up to 11.01% with the optimized NH_4SCN addition at n = 5 [67]. In the same year, Chunqing Ma and co-workers fabricated a 2D-PSC with the device configuration ITO/PEDOT:PSS/$PDAMA_3Pb_4I_{13}$/C_{60}/BCP/Ag and recorded an efficiency of 13% with $PDAMA_3Pb_4I_{13}$ (PDM: propane-1,3-diammonium) as the 2D-perovskite layer using p-i-n inverted structure [67].

3.3 Optoelectronic properties

In this subsection, we will discuss some of the 2D-perovskite's optoelectronic properties, like how reducing dimensionality can affect the bandgap, exciton's influence on charge transport, and so on. In the 2D-perovskites, the large-sized organic cation interlayers can restrict or limit the charge carriers. These organic interlayers act as dielectric regulators, determining the electrostatic force on the electron–hole pairs. The alternating arrangement of inorganic sheets and

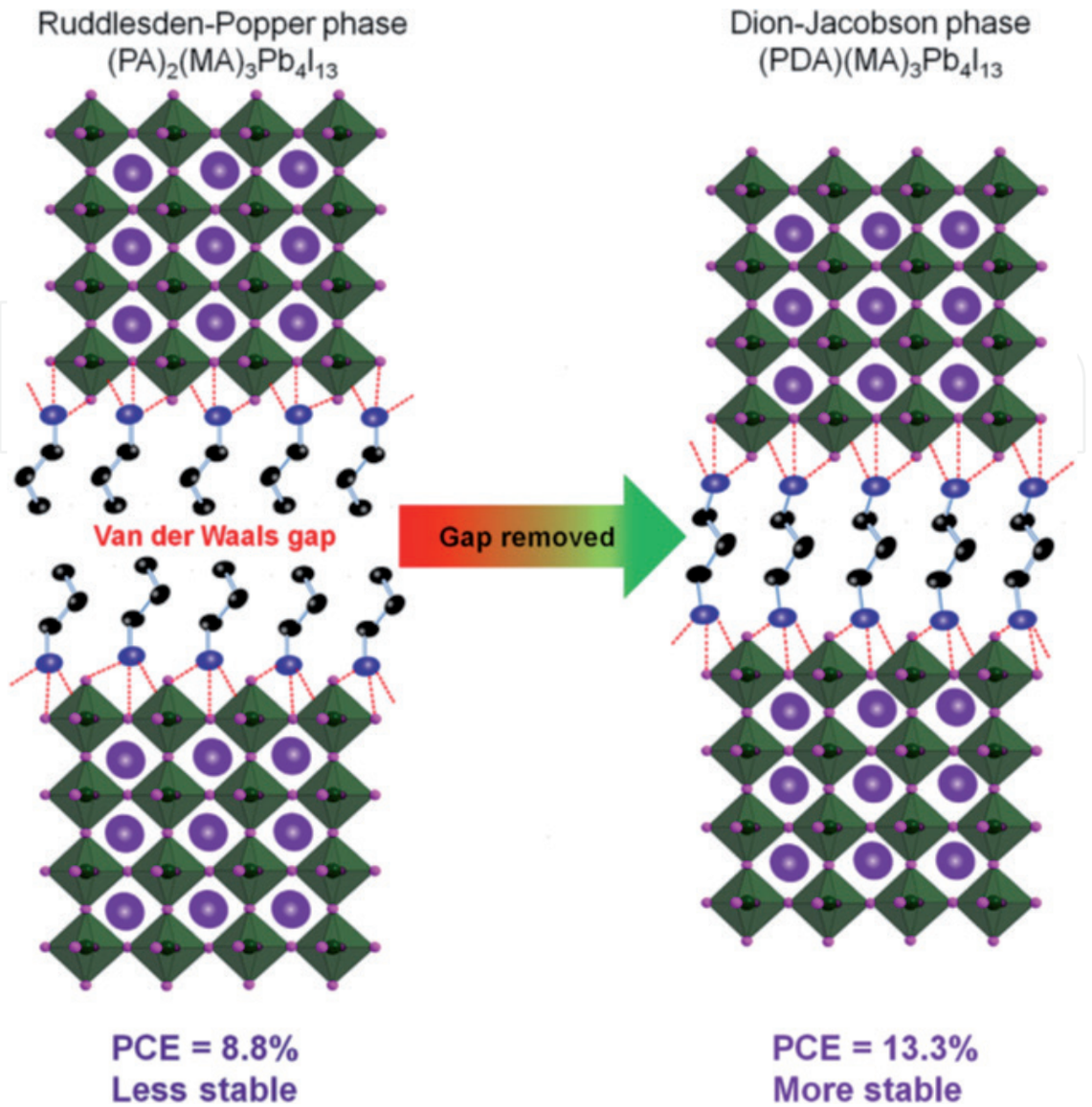

Figure 6.
The D.J. device is more stable and more efficient than the R.P. counterpart. Reprinted with permission from Ref. [64].

bulky organic interlayers results in a multiple-quantum-well (MQW) electronic structure [68]. In other words, the inorganic slabs serve as the potential "wells" while the organic layers function as the potential "barriers" [10] as shown in **Figure 7**. The high organic and inorganic dielectric contrast leads to a huge electron–hole binding energy (Eb) in 2D perovskites [69, 70]. The confinement effect of 2D-perovskites directly affects the bandgap. For an R.P. hybrid perovskite, the bandgap depends on the good width of layer thickness [71]. The total bandgap energy is determined by the base 3D-structure and extra quantization energies of the electron–hole [72]. The optical bandgap of 2D-perovskite generally decreases as the "n" value increases. For example, the bandgap value for the 2D $(CH_3(CH_2)_3NH_3)_2(CH_3NH_3)_{n-1}Pb_nI_{3n+1}$ perovskites decreases with increased layer thickness from 2.24 eV (at n = 1) to 1.52 eV (at n = ∞) due to the quantum-confinement effects associated with the dimensional increase [14]. This flexibility of bandgap tuning can facilitate various optoelectronic applications with targeted optical bandgap materials like tandem solar cells. Those in tandem solar cells, the upper absorber layer needs to have a higher bandgap than the bottom one [73].

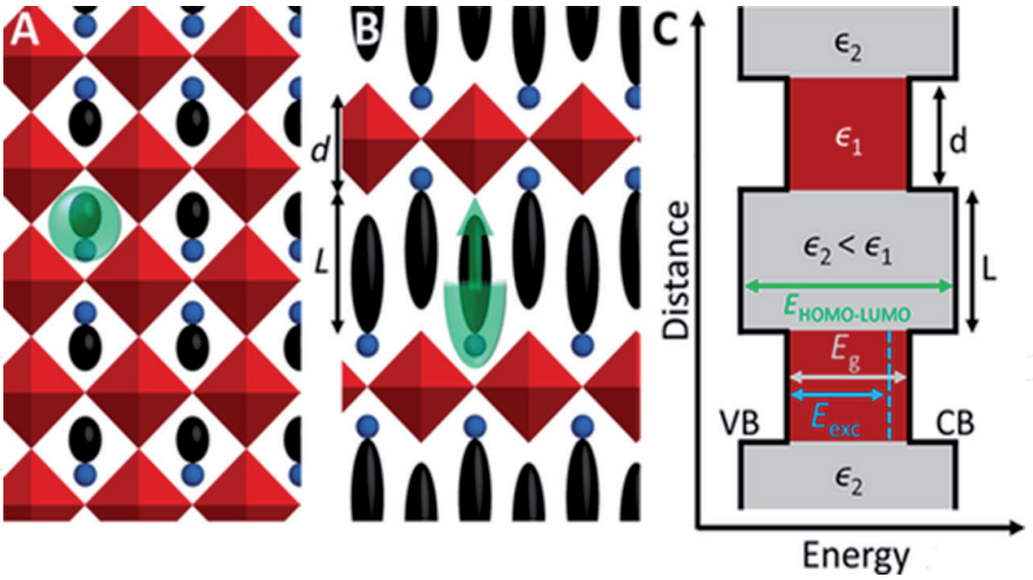

Figure 7.
(A) A schematic of a projection of the 3D-hybrid perovskite, showing an inorganic network of corner-sharing metal halide octahedra (red) with interstitial organic cations (blue, black). (green) highlighting the restriction on cation size. (B) Schematic of a projection down the c-axis of the 2D-hybrid perovskite, showing the alternation of organic (blue, black) and corner-sharing inorganic (red) layers for n = 1 with inorganic layer thickness d and organic layer thickness L. (green), highlighting the restriction solely on the cross-sectional area, but not the length of the organic cation. (C) Energy diagram corresponding to the 2D-structure in (B). Labeling of the valence band (V. B), conduction band (C. B), electronic band gap E_g (gray) and the optical band gap E_{exc} (blue) of the inorganic framework, and the larger HOMO-LUMO gap of the organic cations (green). The organic framework (gray regions) has a dielectric constant ϵ_2, which is smaller than the dielectric constant ϵ_1 of the inorganic framework (red areas). Reprinted with permission from Ref. [70].

Quasi-two-dimensional perovskites have been shown to have strong excitonic effects, and their structure generally shows a large exciton binding energy (E_b) of several hundreds of meV. This improves the interaction between electrons and holes compared to the exchange in 3D-perovskites [74]. The sizeable binding energy E_b in low "n" 2D-perovskites may be detrimental for charge separation in solar cells. So, the considerable binding energy of excitons is one of the main reasons for declining performance standards.

3.4 Device fabrication of 2D-perovskite films

The finite preparation methods of 2D-perovskite films are different from the multiple preparation methods of 3D-perovskite films. *One-step spin-coating methods* are the most used to prepare 2D-perovskite films [75]. In this method, organics and metal halides are dissolved in solvents, e.g., DMF or (DMSO/GBL(1/1)) on substrates. By adjusting the ratio of the precursors, the dimension of perovskite is changed. 2D-perovskite films in both n-i-p and p-i-n structures are fabricated using one-step spin-coating methods as $(PEA)_2(MA)_{n-1}Pb_nI_{3n+1}$, $(BA)_2(MA)_{n-1}Pb_nI_{3n+1}$ and $(PEI)_2(MA)_{n-1}Pb_nI_{3n+1}$ [65, 76, 77]. The *fast deposition-crystallization procedure* was also introduced to fabricate 2D-perovskite by dropping antisolvent, e.g., chlorobenzene, during the spin-coating process. It is shown, homogeneous nuclei are formed immediately and grow up slowly. Finally, dense and uniform films are obtained without oversize grains that may destroy the morphology [78]. The preferred *hot-cast method* was introduced for $(BA)_2(MA)_3Pb_4I_{13}$ films on PEDOT:PSS substrate [66]. The FTO/PEDOT:PSS substrate was heated before the precursor solution was spin-coated on it. **Figure 8** shows the photograph of $(BA)_2(MA)_3Pb_4I_{13}$ films that were prepared on substrates with different hot-cast temperatures from room temperature (R.T.) to 150°C. The films became dark and shiny with lower

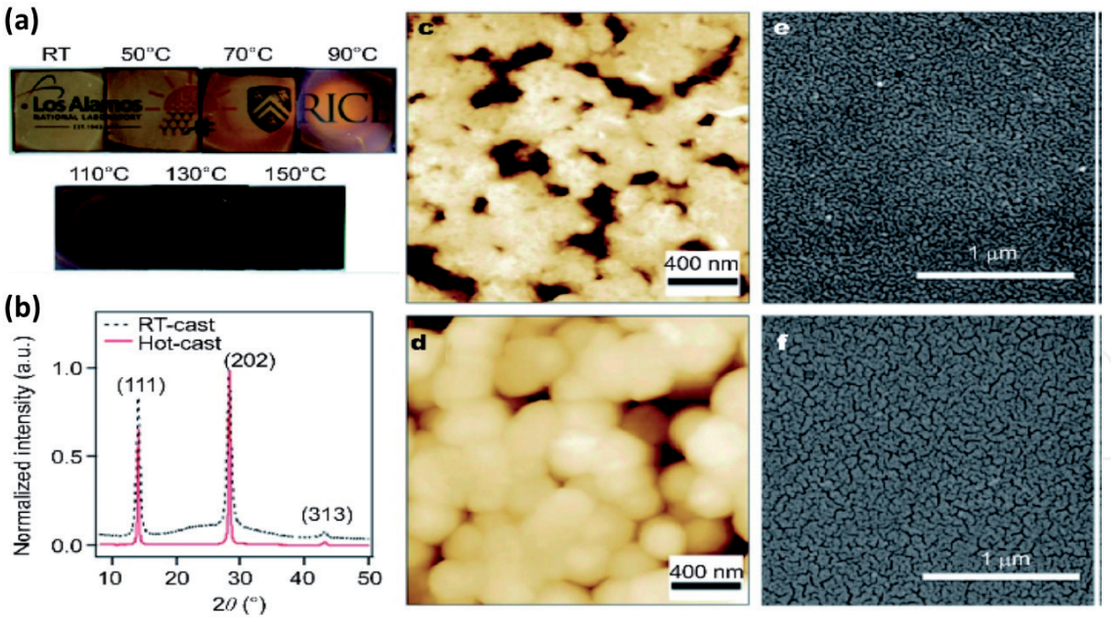

Figure 8.
(a) The $(BA)_2(MA)_3Pb_4I_{13}$ films cast from room temperature (R.T.) to 150°C, (b) GIXRD spectra, (c, d) AFM images, and (e, f) SEM images of films prepared by traditional room-temperature-cast method. Reprinted with permission from Ref. [66].

pinhole density with rising temperature, resulting in high-efficiency devices. The inorganic layers in 2D-perovskite films prepared by the hot-cast method have a preferential orientation vertical to the substrate with excellent crystallinity and few carrier traps, which favors the charge transport.

Another solution vapor annealing method was used to prepare high-quality $(PEA)_2PbBr_4$ nanosheets at room temperature as an emitting layer for LEDs [79]. Using a precursor solution of DMF comprising PEABr and $PbBr_2$ (2/1) was spin-coated on the top of the ITO/PEDOT:PSS substrate and the productive sample was placed face down on the edge of a glass dish without contacting it. In the following step, the dish was transferred into a lidded beaker filled with DMF to form a closed space with DMF vapor at 30°C for several minutes before the DMF vapor diffused under the $(PEA)_2PbI_4$ film and contacted with it. The film was removed out into open air rapidly and heated at 100°C for 10 min while turning into purple. By using DMF vapor annealing, the small and compact $(PEA)_2PbI_4$ perovskite grains was recrystallized into sized nanosheets equally distributed on the substrate, which has larger grain size, higher crystallinity, and higher P.L. intensity (higher photoluminescence quantum yield (PLQY) due to the quantum confinement), comparing with unprocessed films. The nanosheet-LEDs showed a longer P.L. lifetime (much longer than the 3D-perovskite $MAPbI_3$). They exhibited a small leak of current and low turn-on voltage, the external quantum efficiency (EQE) was 20 times higher than poly-LEDs.

Sequential deposition method The sequential deposition is used to prepare a sequential dipping process and sequential spin-coating of 2D-perovskite films [80]. The dipping process was used to fabricate quasi-2D and quasi 3D-perovskite films with spin-coating $(IC_2H_4NH_3)_2PbI_4$ layers on mp-TiO_2 substrates [81]. It is observed, immersing the films into MAI solution with a specific concentration for different times (1–5 min), transferring the films into cleaning fluid (2 mL isopropanol mixed with 10 mL methylbenzene) to remove the MAI residual. With increasing dipping time, MA^+ cations in solution passed through $(IC_2H_4NH_3)_2PbI_4$ films and increased inorganic PbI_4 layers' thickness. Then, the nanoparticles regularly grew up and interconnected with each other in film morphology (uniform films without

residuals), leading to sharper diffraction peaks. In the previous studies, ITO/NiO_x/mixed-dimensional perovskite/PCBM/bis-C_{60}/Ag devices were prepared using the sequential spin-coating method with mixed-cations perovskite $FAxPEA_{1-x}PbI_3$ as the active layer [81]. With observing, a PbI_2 layer was spin-coated on NiO_x substrate, followed by the $PEA_xFA_{1-x}I$ solution loaded on it for 15 s before spin-coating. After thermal treatment, the mixed-cations $FA_xPEA_{1-x}PbI_3$ perovskite films were formed, with migrating PEA^+ cations to lattice surfaces and grain boundaries of 3D-perovskite $FAPbI_3$ to form quasi 3D- rather than quasi 2D-perovskite at room temperature. This self-assembly organic shell could prevent perovskite crystals from ambient moisture and passivated the surface defects to enhance the device performance and quasi 3D-perovskite's stability (the transition energy transformed from black phase to yellow phase). In summary, the 2D-perovskite films were commonly fabricated using one-step spin-coating method (simple process and low cost), with small-n members contrary to their 3D-counterparts but increasing "n" showed pre- or post-treatment is necessary such as hot-cast, antisolvent or solution vapor annealing processes for better crystallization. On the other hand, sequential deposition was used for obtaining efficient charge collection and extraction, dense and uniform films (due to the superior PbI_2 framework for crystal growth). In sequential spin-coating, the large cations were not likely to enter into the lattice but pack on the surface of 3D-perovskite grains, forming a quasi 3D-structure. For future large-scale fabrication, the solution process was not enough for high-quality. Still, doctor blading, pressure-processing method, and so on were more appropriate as long as high-quality crystal is needed [82]. Melt processing is another innovative technique with an excellent quality. It was implemented in 2017 to fabricate lead iodide based 2D-perovskites using PEA derivatives [83]. Although it had not been used for device fabrication yet, however it is a promising one that it exhibits high phase purity, crystallinity, and potential crystal orientation control under ambient air, but its disadvantage is the used toxic solvents in processing.

3.5 Layer orientation

The device performance has been enhanced using the vertical alignment of the inorganic sheets of the 2D-perovskites concerning the substrate. The vertically oriented inorganic slabs provided a direct pathway for charge transport between layers, whereas the bulky organic separators act as electrical insulators hindering out-of-plane conduction of charges [63]. 2D single-layered (n = 1) halide perovskites have shown to align horizontally to the substrate on which they were grown. When "n" was greater than 1, competition arose between horizontal and vertical to the perovskite layers alignment (caused by BA and MA cations). When n = 1–4, it was found that the devices with $n \geq 3$ had a better performance than lower "n", as shown in previous studies [84, 85]. It showed that for $BA_2MA_3Pb_4I_{13}$, the nucleation process and film growth orientation occurred at the liquid-air interface rather than at the liquid–liquid or liquid–substrate interfaces (since surface tension made nucleation and growth at the liquid-air interface more favorable) and that the initial nuclei are oriented in vertical configuration [86]. With increasing "n", the probability of obtaining an n-homogeneous-film decreased, giving rise to a mixture of a 3D-like dominant phase with some 2D-perovskite phases. Finally, films with n = 5–10 tend to align perpendicular to the substrate (**Figure 9**) [87]. This crystal orientation was examined using a scanning electron microscope (SEM), X-ray diffraction (XRD), and grazing incidence wide-angle X-ray scattering (GIWAXS) tests. XRD spectra of $(BA)_2(MA)_{n-1}Pb_nI_{3n+1}$ (n = 1, 2, 3, 4, ∞), with (n = 1) showed (00 k) peaks implying the preferential growth along (110) direction, in (n = 2), (0 k0) reflections occurred in addition to (111) and (222) in

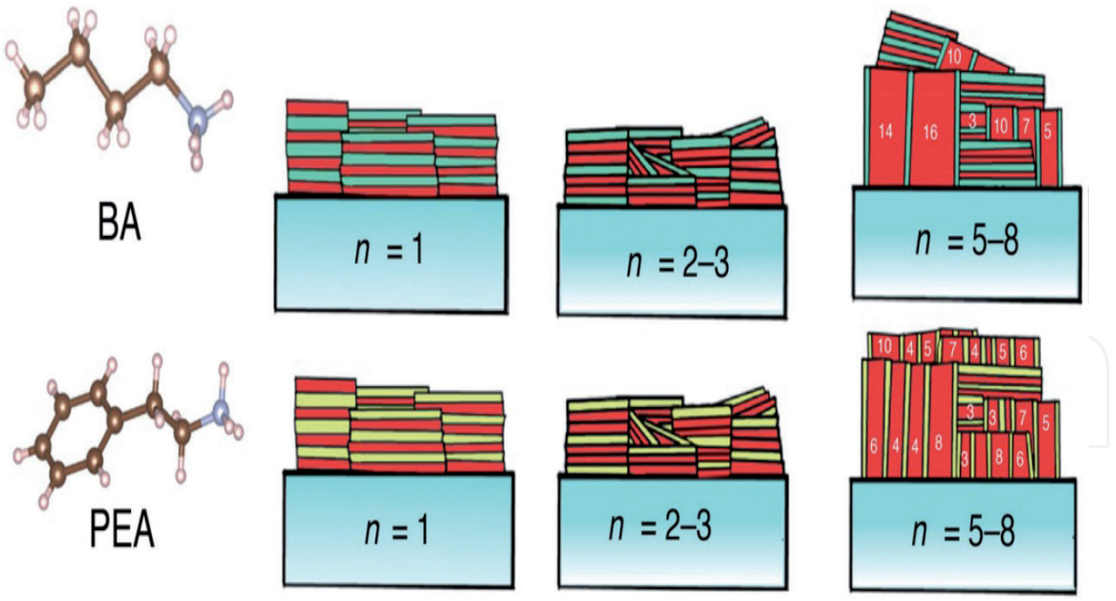

Figure 9.
The generalized concept of the Q.W. morphology in both PEA-based and BA-based spin-cast films. Reprinted with permission from Ref. [87].

the obtained XRD spectra corresponding to in-plane and out-of-plane orientations. In contrast, (111) and (222) reflections were noticed for n = 3 and n = 4 quasi 2D-perovskite films (110) and (220) analogously for n = ∞, which implies the vertical growth orientation (n = 3, 4), increasing towards 3D-perovskite; The preferential layer alignment vanished because few BA cations doped in 3D-perovskite and no influence on orientations **(Figure 9)** [65]. From (SEM, GIWAXS) it was concluded that the hot-cast films grew along certain orientations, confirmed by the most remarkable reflections of (111) and (202) planes. The inorganic crystal plates $<(MA)_{n-1}Pb_nI3_{n+1}>^{2-}$ are perpendicular to the substrate, forming continuous charge transfer channels favorable to charge transport for optoelectronic applications [66].

4. Mixed 2D/3D perovskites

Downsides of 2D-perovskites can be reduced by mixing 2D with the ordinary 3D-perovskites to form 2D/3D perovskite. 2D/3D designing intends to combine the advantages of 3D-perovskite (high optoelectronic properties) and 2D-perovskite (high stability) [88] to produce an efficient and stable perovskite material that could contribute to the advancement of PSCs towards commercial industrialization. So, owing to these reasons, the 2D/3D perovskite attracted the researcher's attention during the last few years [89].

4.1 Optoelectronic properties

The 2D/3D, in comparison to 2D-perovskite, has higher charge mobility, less non-radiative charge recombination, smaller bandgap as illustrated in **Figure 10**, higher power conversion efficiency, long-term stability, and in some cases, do not even need encapsulation.

The number of inorganic layers (n) affects the performance parameters of 2D/3D perovskite. The higher the (n) number, the better the performance

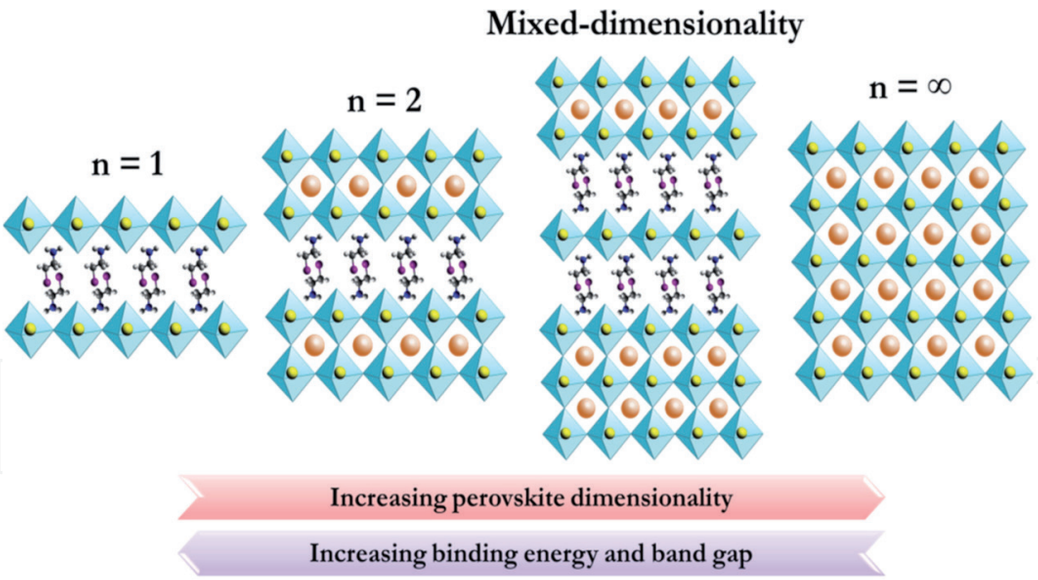

Figure 10.
A schematic illustrates the effect of increasing the dimensionality on the bandgap and the binding energy. Reprinted with permission from Ref. [89].

parameters (as the 2D/3D perovskite gets closer to 3D). Moreover, 2D in 2D/3D can work as a capping layer to protect the 3D layer from air, moisture, heat; It serves as a hydrophobic encapsulation layer. In 2014, Karunadasa et al. introduced the mixed dimensional perovskite in the PSCs for the first time [77]. In this work [77], a mixture of phenylethylammonium (PEA) and MA cations was prepared to obtain a Ruddlesden–Popper structure of $(PEA)_2(MA)_2[Pb_3I_{10}]$ at (n = 3) with an achieved efficiency of 4.73% [77]. The bandgap of the corresponding 2D and 3D-perovskite was 2.10, and 1.63 eV, respectively. After that, Sargent et al. investigated the efficiency and stability of $(PEA)_2(MA)n_{-1}[PbnI_3n_{+1}]$ perovskites with higher n (n = 6, 10, 40, 60, and ∞) [78], the stability of this 2D/3D perovskites was improved compared to the 3D equivalents. The encapsulated device with lower value of n (i.e., closer to 2D) has the highest stability, but the devices with n < 40 have poor performances due to the lower carrier mobility and high radiative recombination losses. For perovskites with (n < 10), a wider bandgap and lower carrier transport lead to inferior performances. On the other hand, the perovskite with (n = 60) recorded the best efficiency (η =15.3%).

4.2 Device fabrication methods

The 2D/3D multidimensional perovskite can be synthesized via many ways: one-step deposition, two-step deposition, anti-solvent method, the self-assembly method, vapor-assisted solution deposition approach [90], etc. In the one-step deposition process, the 2D and 3D precursors are mixed, and the layers are grown simultaneously. In a two-step process, the 3D layer is first deposited then the 2D-perovskite is grown on top of it in a consecutive step. In 2019, Zhang and his co-workers reported a 2D/3D perovskite by post-treated n-butylamine iodide (BAI) and the residual PbI_2 on a one-step deposited $MAPbI_3$ film. They added a thin 2D-perovskite layer on the top of the 3D-perovskite and grain boundaries. The formed 2D/3D perovskite has the stability of 2D (after three months the perovskite still support 80% of its initial efficiency) and the high performance of 3D (V_{OC} = 1.09 V, J_{SC} = 22.55 mA/cm^2 a, FF =0.74, PCE = 18.3%) [91]. The anti-solvent method has been used as an ordinary recipe for getting a 3D-perovskite film [92]. The anti-solvent (e.g., C.B., toluene, etc.)

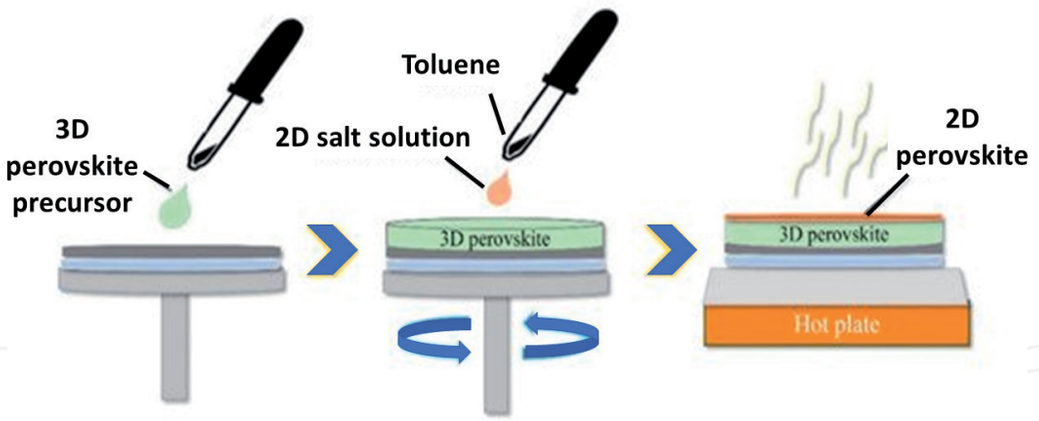

Figure 11.
The process of the anti-solvent method. Reprinted with permission from Ref. [40].

is employed as a second solvent to cause instantaneous nucleation for the 3D film's fast crystallization. When the anti-solvent is used as a solvent for the 2D organic salt, the in-situ 2D growth method can be practically combined with the usual anti-solvent method, as illustrated in **Figure 11**. The anti-solvent containing the organic salt for 2D is directly dripped on the substrate, which is wet with a precursor solution of the 3D-perovskite. The dripping process of the anti-solvent is followed by a one-step process. Toluene containing phenylethylammonium iodide (PEAI) was used as the anti-solvent for a 3D/2D perovskite structure [93].

In the low-pressure vapor assisted solution process, the larger organohalide (PEA) doped with a metal halide (PbI_2) is first spin-coated on the substrate and then reacts with the smaller organohalide (MAI) vapor in a low-pressure oven [94].

4.3 Applications in regular or inverted structure perovskite solar cells

Planer structures are always employed, n-i-p standard structure and p-i-n inverted structure. The researchers used 2D/3D perovskite in these two structures as follows: In 2019, Abbas and his co-workers [95] developed a way to add a 2D-layered perovskite with $MAPbI_3$ bulk 3D-perovskite by a vertically oriented 2D-layered mixed with a bulk 3D-perovskite they select the anilinium ion as the sizeable organic cation. In this research, they used a normal n-i-p structure and recorded an efficiency up to 16%. The planar solar cell heterojunction with ITO/PEDOT-PSS/perovskite/PCBM/BCP/Ag was fabricated [95]. In 2020, Jia Zhang and Bin Hu recorded a 15.93% efficiency with 2D/3D Pb-Sn alloyed perovskite. They applied the inverted structure p-i-n on their work with the solar cell structure (ITO/PEDOT:PSS/$PEA_xMA_{1x}Pb_{0.5}Sn_{0.5}I_3$/$PC_{61}$BM/PEI/Ag) [96].

5. Conclusion

Multi-dimensional 2D/3D hybrid perovskites have proven to be one of the most promising approaches to improving PCE and stability than pure 3D PSCs. Many novel 2D-perovskites can be synthesized in terms of materials engineering and consistent unknown properties studied. Besides, the recently proposed computational theoretical study would speed up selecting and applying 2D materials. In particular, long-chain alkyl cations seem to be suitable for stabilizing perovskite materials based on 2D-Pb-Sn or Sn. The performance can be improved by technical composition and structure. Besides, it remains essential to study the mechanism of

formation of 2D-perovskite layers, which allows us to produce 2D-perovskites with high phase purity and out-of-plane orientation and to cultivate 2D/3D perovskite materials in a more controllable approach. Also, a thorough understanding of the chemical or physical interaction between 2D and 3D perovskite materials, 2D/3D perovskite materials, and neighboring charge transport layers will help achieve efficient and stable PSCs. As the bandgap increases, 2D-perovskite could be ideal for tandem solar cells to drive energy generation. In summary, the development strategy for multi-dimensional 2D/3D perovskites offers an opportunity for efficient and stable PSCs that enable ingenious modification of PSCs and inform their future marketing.

Acknowledgements

The authors acknowledge Science and Technology Development Fund (STDF) and (CMRDI) for their support to this study through the project grant no. 25250 in Egypt.

Conflict of interest

The authors declare no conflict of interest.

Author details

Alaa E. Abd El-Samad[1,2], Radwa S. Mostafa[1], Hager H. Zeenelabden[1,2], Menahtullah M. Mabrouk[3], Ahmed Mourtada Elseman[1*], Nasr Gad[2], Mostafa El-Aasser[2] and Mohamed M. Rashad[1]

1 Electronic and Magnetic Materials Department, Advanced Materials Division, Central Metallurgical Research and Development Institute (CMRDI), Cairo, Egypt

2 Faculty of Science, Physics Department, Ain Shams University, Cairo, Egypt

3 Faculty of Computer Science, Physics Department, Ain Shams University, Cairo, Egypt

*Address all correspondence to: amourtada@cmrdi.sci.eg

IntechOpen

© 2021 The Author(s). Licensee IntechOpen. This chapter is distributed under the terms of the Creative Commons Attribution License (http://creativecommons.org/licenses/by/3.0), which permits unrestricted use, distribution, and reproduction in any medium, provided the original work is properly cited. CC BY

References

[1] Stranks SD, Eperon GE, Grancini G, Menelaou C, Alcocer MJ, Leijtens T, et al. Electron-hole diffusion lengths exceeding 1 micrometer in an organometal trihalide perovskite absorber. Science. 2013;342(6156): 341-344.

[2] Sum TC, Mathews N, Xing G, Lim SS, Chong WK, Giovanni D, et al. Spectral features and charge dynamics of lead halide perovskites: origins and interpretations. Acc Chem Res. 2016;49(2):294-302.

[3] De Wolf S, Holovsky J, Moon S-J, Löper P, Niesen B, Ledinsky M, et al. Organometallic halide perovskites: sharp optical absorption edge and its relation to photovoltaic performance. The journal of physical chemistry letters. 2014;5(6):1035-1039.

[4] Xu CY, Hu W, Wang G, Niu L, Elseman AM, Liao L, et al. Coordinated Optical Matching of a Texture Interface Made from Demixing Blended Polymers for High-Performance Inverted Perovskite Solar Cells. ACS Nano. 2020;14(1):196-203.

[5] Wang G, Liao LP, Elseman AM, Yao YQ, Lin CY, Hu W, et al. An internally photoemitted hot carrier solar cell based on organic-inorganic perovskite. Nano Energy. 2020;68:104383.

[6] Selim MS, Elseman AM, Hao Z. ZnO Nanorods: An Advanced Cathode Buffer Layer for Inverted Perovskite Solar Cells. ACS Applied Energy Materials. 2020;3(12):11781-11791.

[7] Elseman AM, Zaki AH, Shalan AE, Rashad MM, Song QL. TiO2 Nanotubes: An Advanced Electron Transport Material for Enhancing the Efficiency and Stability of Perovskite Solar Cells. Industrial & Engineering Chemistry Research. 2020;59(41):18549-18557.

[8] Elseman AM, Xu C, Yao Y, Elisabeth M, Niu L, Malavasi L, et al. Electron Transport Materials: Evolution and Case Study for High-Efficiency Perovskite Solar Cells. Solar RRL. 2020;4(7):2000136.

[9] Elseman AM, Luo L, Song QL. Self-doping synthesis of trivalent Ni2O3 as a hole transport layer for high fill factor and efficient inverted perovskite solar cells. Dalton Transactions. 2020;49(40):14243-14250.

[10] Yang XD, Han JJ, Wang G, Liao LP, Xu CY, Hu W, et al. Robust perovskite-based triboelectric nanogenerator enhanced by broadband light and interface engineering. Journal of Materials Science. 2019;54(12): 9004-9016.

[11] Sanad MMS, Elseman AM, Elsenety MM, Rashad MM, Elsayed BA. Facile synthesis of sulfide-based chalcogenide as hole-transporting materials for cost-effective efficient perovskite solar cells. Journal of Materials Science: Materials in Electronics. 2019;30(7):6868-6875.

[12] Sajid S, Elseman AM, Wei D, Ji J, Dou S, Huang H, et al. NiO@carbon spheres: A promising composite electrode for scalable fabrication of planar perovskite solar cells at low cost. Nano Energy. 2019;55:470-476.

[13] Sajid S, Elseman AM, Wei D, Ji J, Dou S, Huang H, et al. Corrigendum to "NiO@Carbon spheres: A promising composite electrode for scalable fabrication of planar perovskite solar cells at low cost" [Nano Energy, 55 (2019) 470-476]. Nano Energy. 2019;58:94-95.

[14] Liu DB, Wang G, Niu LB, Chen LJ, Liu DY, Rao X, et al. Energy Level Bending of Organic-Inorganic Halide Perovskite by Interfacial Dipole. physica

status solidi (RRL) – Rapid Research Letters. 2019;13(7):1900103.

[15] Hu W, Xu CY, Niu LB, Elseman AM, Wang G, Liu B, et al. High Open-Circuit Voltage of 1.134 V for Inverted Planar Perovskite Solar Cells with Sodium Citrate-Doped PEDOT:PSS as a Hole Transport Layer. ACS Appl Mater Interfaces. 2019;11(24):22021-22027.

[16] Elseman AM, Selim MS, Luo L, Xu CY, Wang G, Jiang Y, et al. Efficient and Stable Planar n-i-p Perovskite Solar Cells with Negligible Hysteresis through Solution-Processed Cu2 O Nanocubes as a Low-Cost Hole-Transport Material. ChemSusChem. 2019;12(16):3808-16.

[17] Elseman AM, Sajid S, Shalan AE, Mohamed SA, Rashad MM. Recent progress concerning inorganic hole transport layers for efficient perovskite solar cells. Appl Phys A. 2019;125(7).

[18] Wei D, Ma F, Wang R, Dou S, Cui P, Huang H, et al. Ion-Migration Inhibition by the Cation-pi Interaction in Perovskite Materials for Efficient and Stable Perovskite Solar Cells. Adv Mater. 2018;30(31):e1707583.

[19] Shalan AE, Barhoum A, Elseman AM, Rashad MM, Lira-Cantú M. Nanofibers as Promising Materials for New Generations of Solar Cells. In: Barhoum A, Bechelany M, Makhlouf A, editors. Handbook of Nanofibers. Cham: Springer International Publishing; 2018. p. 1-33.

[20] Sajid S, Elseman AM, Ji J, Dou S, Wei D, Huang H, et al. Computational Study of Ternary Devices: Stable, Low-Cost, and Efficient Planar Perovskite Solar Cells. Nano-Micro Letters. 2018;10(3).

[21] Sajid S, Elseman AM, Huang H, Ji J, Dou S, Jiang H, et al. Breakthroughs in NiOx-HTMs towards stable, low-cost and efficient perovskite solar cells. Nano Energy. 2018;51:408-424.

[22] Sajid AME, Jun Ji, Shangyi Dou, Hao Huang, Peng Cui, Dong Wei, Meicheng Li. Novel hole transport layer of nickel oxide composite with carbon for high-performance perovskite solar cells. Chin Phys B. 2018;27(1): 17305-017305.

[23] Elseman AM, Sharmoukh W, Sajid S, Cui P, Ji J, Dou S, et al. Superior Stability and Efficiency Over 20% Perovskite Solar Cells Achieved by a Novel Molecularly Engineered Rutin-AgNPs/Thiophene Copolymer. Adv Sci (Weinh). 2018;5(11):1800568.

[24] Elseman AM, Shalan AE, Sajid S, Rashad MM, Hassan AM, Li M. Copper-Substituted Lead Perovskite Materials Constructed with Different Halides for Working (CH3NH3)2CuX4-Based Perovskite Solar Cells from Experimental and Theoretical View. ACS Appl Mater Interfaces. 2018;10(14):11699-11707.

[25] Elseman AM. Organometal halide perovskites thin film and their impact on the efficiencyof perovskite solar cells. Coatings and Thin-Film Technologies: IntechOpen; 2018.

[26] Elseman AM, Shalan AE, Rashad MM, Hassan AM. Experimental and simulation study for impact of different halides on the performance of planar perovskite solar cells. Mater Sci Semicond Process. 2017;66:176-185.

[27] Rashad MM, Elseman AM, Hassan AM. Facile synthesis, characterization and structural evolution of nanorods single-crystalline (C4H9NH3)2PbI2X2 mixed halide organometal perovskite for solar cell application. Optik. 2016;127(20): 9775-9787.

[28] Elseman AM, Rashad MM, Hassan AM. Easily Attainable, Efficient Solar Cell with Mass Yield of Nanorod Single-Crystalline Organo-Metal Halide Perovskite Based on a Ball Milling

Technique. ACS Sustainable Chemistry & Engineering. 2016;4(9):4875-4886.

[29] Saparov B, Mitzi DB. Organic–inorganic perovskites: structural versatility for functional materials design. Chem Rev. 2016;116(7): 4558-4596.

[30] Wells A. Structural Inorganic Chemistry, 739 Oxford. UK: Clarendon Press; 1984.

[31] Teale S, Proppe A, Jung EH, Johnston A, Parmar DH, Chen B, et al. Dimensional Mixing Increases the Efficiency of 2D/3D Perovskite Solar Cells. The Journal of Physical Chemistry Letters. 2020.

[32] Jiang P, Xiong Y, Xu M, Mei A, Sheng Y, Hong L, et al. The influence of the work function of hybrid carbon electrodes on printable mesoscopic perovskite solar cells. The Journal of Physical Chemistry C. 2018;122(29):16481-16487.

[33] Leguy AM, Hu Y, Campoy-Quiles M, Alonso MI, Weber OJ, Azarhoosh P, et al. Reversible hydration of CH3NH3PbI3 in films, single crystals, and solar cells. Chem Mater. 2015;27(9):3397-3407.

[34] Christians JA, Miranda Herrera PA, Kamat PV. Transformation of the excited state and photovoltaic efficiency of CH3NH3PbI3 perovskite upon controlled exposure to humidified air. J Am Chem Soc. 2015;137(4):1530-1538.

[35] Urbani M, de la Torre G, Nazeeruddin MK, Torres T. Phthalocyanines and porphyrinoid analogues as hole-and electron-transporting materials for perovskite solar cells. Chem Soc Rev. 2019;48(10):2738-2766.

[36] Wang H, Zhao Y, Wang Z, Liu Y, Zhao Z, Xu G, et al. Hermetic seal for perovskite solar cells: An improved plasma enhanced atomic layer deposition encapsulation. Nano Energy. 2020;69:104375.

[37] Meng H, Shao Z, Wang L, Li Z, Liu R, Fan Y, et al. Chemical composition and phase evolution in DMAI-derived inorganic perovskite solar cells. ACS Energy Letters. 2019;5(1):263-270.

[38] Kang Y-J, Kwon S-N, Cho S-P, Seo Y-H, Choi M-J, Kim S-S, et al. Antisolvent additive engineering containing dual-function additive for triple-cation p–i–n perovskite solar cells with over 20% PCE. ACS Energy Letters. 2020;5(8):2535-2545.

[39] Yao Q, Xue Q, Li Z, Zhang K, Zhang T, Li N, et al. Graded 2D/3D Perovskite Heterostructure for Efficient and Operationally Stable MA-Free Perovskite Solar Cells. Adv Mater. 2020:2000571.

[40] Choi H-S, Kim H-S. 3D/2D bilayerd perovskite solar cells with an enhanced stability and performance. Materials. 2020;13(17):3868.

[41] Jodlowski AD, Roldán-Carmona C, Grancini G, Salado M, Ralaiarisoa M, Ahmad S, et al. Large guanidinium cation mixed with methylammonium in lead iodide perovskites for 19% efficient solar cells. Nature Energy. 2017;2(12):972-979.

[42] Grancini G, Roldán-Carmona C, Zimmermann I, Mosconi E, Lee X, Martineau D, et al. One-Year stable perovskite solar cells by 2D/3D interface engineering. Nature communications. 2017;8(1):1-8.

[43] Ortiz-Cervantes C, Carmona-Monroy P, Solis-Ibarra D. Two-Dimensional Halide Perovskites in Solar Cells: 2D or not 2D? ChemSusChem. 2019;12(8):1560-1575.

[44] Chen P, Bai Y, Lyu M, Yun JH, Hao M, Wang L. Progress and

Perspective in Low-Dimensional Metal Halide Perovskites for Optoelectronic Applications. Solar Rrl. 2018;2(3):1700186.

[45] Misra RK, Cohen BE, Iagher L, Etgar L. Low-dimensional organic–inorganic halide perovskite: structure, properties, and applications. Chem SusChem. 2017;10(19):3712-3721.

[46] Slavney AH, Smaha RW, Smith IC, Jaffe A, Umeyama D, Karunadasa HI. Chemical approaches to addressing the instability and toxicity of lead–halide perovskite absorbers. Inorg Chem. 2017;56(1):46-55.

[47] Rodríguez-Romero J, Sanchez-Diaz J, Echeverría-Arrondo C, Masi S, Esparza D, Barea EM, et al. Widening the 2D/3D Perovskite Family for Efficient and Thermal-Resistant Solar Cells by the Use of Secondary Ammonium Cations. ACS Energy Letters. 2020;5(4):1013-1021.

[48] Wang Z, Lin Q, Chmiel FP, Sakai N, Herz LM, Snaith HJ. Efficient ambient-air-stable solar cells with 2D–3D heterostructured butylammonium-caesium-formamidinium lead halide perovskites. Nature Energy. 2017;2(9):17135.

[49] Di Giacomo F, Fakharuddin A, Jose R, Brown TM. Progress, challenges and perspectives in flexible perovskite solar cells. Energy & Environmental Science. 2016;9(10):3007-3035.

[50] Lu C-H, Biesold-McGee GV, Liu Y, Kang Z, Lin Z. Doping and ion substitution in colloidal metal halide perovskite nanocrystals. Chem Soc Rev. 2020;49(14):4953-5007.

[51] Dong H, Wu Z, Xi J, Xu X, Zuo L, Lei T, et al. Pseudohalide-Induced Recrystallization Engineering for CH3NH3PbI3 Film and Its Application in Highly Efficient Inverted Planar Heterojunction Perovskite Solar Cells. Adv Funct Mater. 2018;28(2):1704836.

[52] Gu S, Lin R, Han Q, Gao Y, Tan H, Zhu J. Tin and mixed lead–tin halide perovskite solar cells: progress and their application in tandem solar cells. Adv Mater. 2020:1907392.

[53] Selim MS, Elseman AM, Hao Z. ZnO Nanorods: An Advanced Cathode Buffer Layer for Inverted Perovskite Solar Cells. ACS Applied Energy Materials. 2020.

[54] Wang DN, White JM, Law KS, Leung C, Umotoy SP, Collins KS, et al. Thermal CVD/PECVD reactor and use for thermal chemical vapor deposition of silicon dioxide and in-situ multi-step planarized process. Google Patents; 1991.

[55] Meléndrez M, Solis-Pomar F, Gutierrez-Lazos C, Flores P, Jaramillo A, Fundora A, et al. A new synthesis route of ZnO nanonails via microwave plasma-assisted chemical vapor deposition. Ceram Int. 2016;42(1):1160-1168.

[56] Shahidi S, Moazzenchi B, Ghoranneviss M. A review-application of physical vapor deposition (PVD) and related methods in the textile industry. The European Physical Journal Applied Physics. 2015;71(3):31302.

[57] Grancini G, Nazeeruddin MK. Dimensional tailoring of hybrid perovskites for photovoltaics. Nature Reviews Materials. 2019;4(1):4-22.

[58] Lin H, Zhou C, Tian Y, Siegrist T, Ma B. Low-dimensional organometal halide perovskites. ACS Energy Letters. 2017;3(1):54-62.

[59] Shi E, Gao Y, Finkenauer BP, Coffey AH, Dou L. Two-dimensional halide perovskite nanomaterials and heterostructures. Chem Soc Rev. 2018;47(16):6046-6072.

[60] Gan X, Wang O, Liu K, Du X, Guo L, Liu H. 2D homologous organic-inorganic hybrids as light-absorbers for planer and nanorod-based perovskite solar cells. Sol Energy Mater Sol Cells. 2017;162:93-102.

[61] Zhang F, Lu H, Tong J, Berry JJ, Beard MC, Zhu K. Advances in two-dimensional organic–inorganic hybrid perovskites. Energy & Environmental Science. 2020;13(4):1154-1186.

[62] Chen Y, Yu S, Sun Y, Liang Z. Phase engineering in quasi-2D Ruddlesden–Popper perovskites. The journal of physical chemistry letters. 2018;9(10):2627-2631.

[63] Mao L, Ke W, Pedesseau L, Wu Y, Katan C, Even J, et al. Hybrid Dion–Jacobson 2D lead iodide perovskites. J Am Chem Soc. 2018;140(10): 3775-3783.

[64] Ahmad S, Fu P, Yu S, Yang Q, Liu X, Wang X, et al. Dion-Jacobson phase 2D layered perovskites for solar cells with ultrahigh stability. Joule. 2019;3(3):794-806.

[65] Cao DH, Stoumpos CC, Farha OK, Hupp JT, Kanatzidis MG. 2D homologous perovskites as light-absorbing materials for solar cell applications. J Am Chem Soc. 2015;137(24):7843-7850.

[66] Tsai H, Nie W, Blancon J-C, Stoumpos CC, Asadpour R, Harutyunyan B, et al. High-efficiency two-dimensional Ruddlesden–Popper perovskite solar cells. Nature. 2016;536(7616):312-316.

[67] Zhang X, Wu G, Fu W, Qin M, Yang W, Yan J, et al. Orientation regulation of phenylethylammonium cation based 2D perovskite solar cell with efficiency higher than 11%. Advanced Energy Materials. 2018;8(14):1702498.

[68] Davy MM, Jadel TM, Qin C, Luyun B, Mina G. Recent progress in low dimensional (quasi-2D) and mixed dimensional (2D/3D) tin-based perovskite solar cells. Sustainable Energy & Fuels. 2020.

[69] Guo Z, Wu X, Zhu T, Zhu X, Huang L. Electron–phonon scattering in atomically thin 2D perovskites. ACS nano. 2016;10(11):9992-9998.

[70] Straus DB, Kagan CR. Electrons, excitons, and phonons in two-dimensional hybrid perovskites: connecting structural, optical, and electronic properties. The journal of physical chemistry letters. 2018;9(6):1434-1447.

[71] Gao P, Nazeeruddin MK. Dimensionality engineering of hybrid halide perovskite light absorbers. Nature communications. 2018;9(1):1-14.

[72] Sichert JA, Tong Y, Mutz N, Vollmer M, Fischer S, Milowska KZ, et al. Quantum size effect in organometal halide perovskite nanoplatelets. Nano Lett. 2015;15(10):6521-6527.

[73] Pohle L. US photovoltaic patents: 1991--1993. National Renewable Energy Lab., Golden, CO (United States); 1995.

[74] Manser JS, Christians JA, Kamat PV. Intriguing optoelectronic properties of metal halide perovskites. Chem Rev. 2016;116(21):12956-13008.

[75] Cortecchia D, Dewi HA, Yin J, Bruno A, Chen S, Baikie T, et al. Lead-free MA2CuCl x Br4–x hybrid perovskites. Inorg Chem. 2016;55(3):1044-1052.

[76] Yao K, Wang X, Xu Y-x, Li F, Zhou L. Multilayered perovskite materials based on polymeric-ammonium cations for stable large-area solar cell. Chem Mater. 2016;28(9): 3131-3138.

[77] Smith IC, Hoke ET, Solis-Ibarra D, McGehee MD, Karunadasa HI. A layered hybrid perovskite solar-cell absorber with enhanced moisture stability. Angew Chem. 2014;126(42): 11414-11417.

[78] Quan LN, Yuan M, Comin R, Voznyy O, Beauregard EM, Hoogland S, et al. Ligand-stabilized reduced-dimensionality perovskites. J Am Chem Soc. 2016;138(8):2649-2655.

[79] Liang D, Peng Y, Fu Y, Shearer MJ, Zhang J, Zhai J, et al. Color-pure violet-light-emitting diodes based on layered lead halide perovskite nanoplates. ACS nano. 2016;10(7): 6897-6904.

[80] Li N, Zhu Z, Chueh CC, Liu H, Peng B, Petrone A, et al. Mixed cation FAxPEA1–xPbI3 with enhanced phase and ambient stability toward high-performance perovskite solar cells. Advanced Energy Materials. 2017;7(1):1601307.

[81] Koh TM, Shanmugam V, Schlipf J, Oesinghaus L, Müller-Buschbaum P, Ramakrishnan N, et al. Nanostructuring mixed-dimensional perovskites: a route toward tunable, efficient photovoltaics. Adv Mater. 2016;28(19):3653-3661.

[82] Ma S, Cai M, Cheng T, Ding X, Shi X, Alsaedi A, et al. Two-dimensional organic-inorganic hybrid perovskite: from material properties to device applications. Science China Materials. 2018;61(10):1257-1277.

[83] Li T, Dunlap-Shohl WA, Han Q, Mitzi DB. Melt processing of hybrid organic–inorganic lead iodide layered perovskites. Chem Mater. 2017;29(15):6200-6204.

[84] Tsai H, Asadpour R, Blancon J-C, Stoumpos CC, Even J, Ajayan PM, et al. Design principles for electronic charge transport in solution-processed vertically stacked 2D perovskite quantum wells. Nature communications. 2018;9(1):1-9.

[85] Liao Y, Liu H, Zhou W, Yang D, Shang Y, Shi Z, et al. Highly oriented low-dimensional tin halide perovskites with enhanced stability and photovoltaic performance. J Am Chem Soc. 2017;139(19):6693-6699.

[86] Quintero-Bermudez R, Gold-Parker A, Proppe AH, Munir R, Yang Z, Kelley SO, et al. Compositional and orientational control in metal halide perovskites of reduced dimensionality. Nature materials. 2018;17(10):900-907.

[87] Wu C-G, Chiang C-H, Chang SH. A perovskite cell with a record-high-V oc of 1.61 V based on solvent annealed CH 3 NH 3 PbBr 3/ICBA active layer. Nanoscale. 2016;8(7):4077-4085.

[88] Gharibzadeh S, Abdollahi Nejand B, Jakoby M, Abzieher T, Hauschild D, Moghadamzadeh S, et al. Record Open-Circuit Voltage Wide-Bandgap Perovskite Solar Cells Utilizing 2D/3D Perovskite Heterostructure. Advanced Energy Materials. 2019;9(21):1803699.

[89] Krishna A, Gottis S, Nazeeruddin MK, Sauvage F. Mixed dimensional 2D/3D hybrid perovskite absorbers: the future of perovskite solar cells? Adv Funct Mater. 2019;29(8):1806482.

[90] Yusoff ARbM, Nazeeruddin MK. Low-Dimensional Perovskites: From Synthesis to Stability in Perovskite Solar Cells. Advanced Energy Materials. 2018;8(26):1702073.

[91] Zou Y, Cui Y, Wang H-Y, Cai Q, Mu C, Zhang J-P. Highly efficient and stable 2D–3D perovskite solar cells fabricated by interfacial modification. Nanotechnology. 2019;30(27):275202.

[92] Xiao M, Huang F, Huang W, Dkhissi Y, Zhu Y, Etheridge J, et al. A fast deposition-crystallization

procedure for highly efficient lead iodide perovskite thin-film solar cells. Angew Chem Int Ed. 2014;53(37):9898-9903.

[93] Bai Y, Xiao S, Hu C, Zhang T, Meng X, Lin H, et al. Dimensional Engineering of a Graded 3D–2D Halide Perovskite Interface Enables Ultrahigh Voc Enhanced Stability in the p-i-n Photovoltaics. Advanced Energy Materials. 2017;7(20):1701038.

[94] Li MH, Yeh HH, Chiang YH, Jeng US, Su CJ, Shiu HW, et al. Highly Efficient 2D/3D Hybrid Perovskite Solar Cells via Low-Pressure Vapor-Assisted Solution Process. Adv Mater. 2018;30(30):1801401.

[95] Abbas MS, Hussain S, Zhang J, Wang B, Yang C, Wang Z, et al. Orientationally engineered 2D/3D perovskite for high efficiency solar cells. Sustainable Energy & Fuels. 2020;4(1):324-330.

[96] Zhang J, Hu B. Revealing photoinduced bulk polarization and spin-orbit coupling effects in high-efficiency 2D/3D Pb–Sn alloyed perovskite solar cells. Nano Energy. 2020;76:104999.

IntechOpen